Interferometric ISAR Imaging Based on Compressive Sensing

Wei Qiu
ATR Key Lab
National University of Defense Technology
Changsha, China
Email: williamqiuwei@gmail.com

Marco Martorella
Department of Information Engineering
University of Pisa
Pisa, Italy
Email: m.martorella@unipi.iet.it

Fabrizio Berizzi
Department of Information Engineering
University of Pisa
Pisa, Italy
Email: f.berizzi@unipi.iet.it

Abstract—**Inverse Synthetic Aperture Radar (ISAR) images are often used for target classification and recognition applications. However, conventional 2D images do not provide the height information about the scattering centers. In this paper, an interferometric ISAR imaging method based on compressive sensing (CS) is proposed that is able to estimate the scatterering centres heights. The interferometric ISAR system we consider is composed of two antennas at closely-separated elevation angles. In this paper, we propose a joint processing of the multichannel data to form ISAR images, which improves the height estimation performance over the case of independent processing. Simulation results are produced in order to verify the effectiveness of the proposed method and to compare with the independent processing.**

Index Terms—**Interferometric ISAR, 3D target reconstruction, Compressive sensing, Multichannel ISAR imaging**

I. INTRODUCTION

Inverse Synthetic Aperture Radar can form 2D electromagnetic images of targets, which are then typically used for target classification and/or recognition. A number of issues are related to the use of 2D-ISAR images for classification and recognition purposes. One of such is the fact that the ISAR Image Projection Plane (IPP) is not known *a priori*. This typically causes a serious difficulty to interpret the ISAR image. One way to overcome this problem is to form 3D ISAR images where the third dimension of the target is retained.

Interferometric ISAR imaging processing has recently been introduced to estimate the height information of imaged target [3] [4]. It should be clarified that the third dimension is produced as an estimation process and therefore the image produced is not a 3D image strictly speaking. Also, the target's height is to be interpreted with respect to the image plane, which is not necessarily parallel to the horizon. The interferometric ISAR technique introduced in [3] [4] exploits the phase difference of the corresponding pixels of two ISAR images produced by two closely separated antennas along the elevation direction to form the locations of the scattering centers in the third dimension. We should also clarify here that a configuration with two antennas does not produce an effective In-ISAR system. This is due to the fact that the IPP is not know *a priori* and therefore the height direction (with respect to the IPP) is not known. Nevertheless, it has been demonstrated in [4] that a configuration with two orthogonal

baseline can effectively solve such problem allowing for both the IPP orientation and the height to be estimated. As the height information should be derived from two ISAR images from two corresponding receivers, a traditional ISAR images formulation utilizes Fourier transforming processing to produce the reflectivity map of the target, but it has inherent resolution limits.

Actually, there are only a few main scattering centers in the whole ISAR imaging plane, which means that the ISAR signal is sparse. This fact motivates the application of compressive sensing (CS) theory [6] [7] to generate ISAR images under the sparsity constraint. In order to preserve the phase information in each ISAR image, the real and imaginary parts of the signal should be processed separately, and then combined to form the final ISAR image of the target. In the case of interferometric ISAR, the data is collected from at least two channels (two antennas), so one way to reconstruct the ISAR images is to apply CS independently for each channel. Such method, although it can produce good ISAR images, it is not effective when using a pair of images to form the interferogram. In fact, the relative phase information may not be preserved on account of the possibility of shifts between the two images. In this paper, by defining a global sparsity of ISAR image pairs, and by defining a CS method that jointly forms CS ISAR images, scattering centers are located in the same pixels in both images. Consequently, the height estimation performance is improved with respect to independent processing. Furthermore, the proposed method can generate 3D imaging result of a target using limited measurements.

This paper is organized as follows: the received signal model is presented in section II. Interferometric ISAR imaging based on CS is illustrated in section III. Simulation results are shown in section IV. Finally, section V concludes this paper and future work is also discussed.

II. SIGNAL MODEL

Consider a simple interferometric ISAR system shown in Figure 1, where two antennas O and A are located separately along the elevation direction, and the target is rotated in the xoy plane. Based on the ideal point-like scatterer model and after motion compensation, the received signal at antenna i (

Figure 1: Interferometric ISAR system geometry

$i \in \{O, A\}$) from a scatterer can be written as:

$$s_i(f_m, \theta_n) = \sigma_i \exp\{ -j\frac{4\pi f_m}{c}(x\cos\theta_n \cos\varphi_i + \tag{1}$$
$$y\sin\theta_n\cos\varphi_i + z\sin\varphi_i)\}$$

where σ_i is the reflectivity of the sactterer, whose coordinate is (x, y, z) at the antenna i, $f_m = f_0 + (m-1)\Delta f$, $m = 1, 2, ..., M$ is the transmitted frequency, $\theta_n = (n-1)\Delta\theta$, $n = 1, 2, ..., N$, is the rotation angle in the image plane, φ_i is the elevation angle from the phase center of the ith antenna to the target center O', and c is the speed of light.

Assuming that the total rotation angle is small during the observation time, and thus $\cos\theta_n \approx 1$, $\cos\theta_n \approx \theta_n = (n-1)\Delta\theta$, equation (1) can be expressed as follows:

$$s_i(f_m, \theta_n) = \sigma_i \exp\{ -j\frac{4\pi f_m}{c}(x\cos\varphi_i + \tag{2}$$
$$y(n-1)\Delta\theta\cos\varphi_i + z\sin\varphi_i)\}$$

The imaging plane can be digitized by $x\cos\varphi_i = p\Delta x$, $y\cos\varphi_i = q\Delta y$, $p = 1, 2, ..., M$, $q = 1, 2, ..., N$, where $\Delta x = \frac{c}{2B} = \frac{c}{M\Delta f}$, $\Delta y = \frac{\lambda}{2N\Delta\theta}$, the equation (2) can be written as:

$$s_i(f_m, \theta_n) = \sum_{p=1}^{M}\sum_{q=1}^{N}\sigma_i(p, q)\exp\{-j\frac{4\pi f_m}{c}z\sin\varphi_i\}$$
$$\exp\{ -2j\pi\frac{p(m-1)}{M}\}\exp\{ -2j\pi\frac{q(n-1)}{N}\} \tag{3}$$

Supposing the bandwidth is sufficiently small with respect to the carrier frequency, we have $\exp\{-j\frac{4\pi f_m}{c}z\sin\varphi_i\} \approx \exp\{-j\frac{4\pi f_0}{c}z\sin\varphi_i\}$, and the ISAR image can be obtained by applying 2D-FT to equation (3).

Furthermore, after interferometric processing, the phase difference of the scatterer between two received signals can be expressed as follows:

$$\Delta\phi \approx \frac{4\pi f_0}{c}z(\sin\varphi_A - \sin\varphi_O) \tag{4}$$

Since the baseline length is much shorter than the distance between the radar and the target, the elevation angle difference of the two antennas is quite small. In the case of this paper,

$\varphi_A = \varphi_O + \Delta\varphi$, and $\Delta\varphi \ll 1$. As a consequence, equation (4) can be written as:

$$\Delta\phi \approx \frac{4\pi f_0}{c}z(\sin(\varphi_O + \Delta\varphi) - \sin\varphi_O)$$
$$\approx \frac{4\pi f_0}{c}z(\sin\varphi_O\cos\Delta\varphi + \cos\varphi_O\sin\Delta\varphi - \sin\varphi_O)$$
$$\approx \frac{4\pi f_0}{c}z\cos\varphi_O\Delta\varphi \tag{5}$$

As a result, the height of the scatterer can be estimated by

$$z \approx \frac{c}{4\pi f_0\cos\varphi_O}\frac{\Delta\phi}{\Delta\varphi} \tag{6}$$

Equation (6) implies that for a target composed of K scattering centers, the height of each scatterer can be formed by the phase difference between the corresponding pixels of two ISAR images from two closely separated antennas located along the elevation direction. In addition, it is worthy noticing that in order to guarantee the height estimation is unambiguous, the baseline length d should satisfy the following upper bounds:

$$d < \frac{cR_0}{2f_0 H} \tag{7}$$

where R_0 is the distance from the radar to the target, H is the projection of the target with the maximum height onto the image plane. We also assume that there is at most one scattering center in one pixel of the Range-Doppler map.

III. CS FOR INTERFEROMETRIC ISAR

In this section, we will propose a CS based interferometric ISAR imaging scheme to form the 3D image of the target.

As the height estimation is taken from a pair of ISAR images produced by two elevation separate antennas, the first step is to generate ISAR images based on CS. By referring to equation (3) and by choosing $p = 1, 2, ..., P$, $q = 1, 2, ..., Q$, $P > M$, $Q > N$, the received signal for each channel can be rewritten as the following matrix form:

$$\mathbf{S}_i = \mathbf{\Phi}_x\mathbf{\Omega}_i\mathbf{\Phi}_y^{\mathrm{T}} \tag{8}$$

where $\mathbf{S}_i$ is data matrix from ith channel with the size of $M \times N$, $\mathbf{\Omega}_i$ with the size of $P \times Q$ denotes the ISAR image to be formed in the ith channel, and $\mathbf{\Phi}_x$ as well as $\mathbf{\Phi}_y$ are $P \times M$ and $Q \times N$ matrices, representing the Fourier dictionaries in the frequency and slow-time domains, respectively. The matrices $\mathbf{\Phi}_x$ and $\mathbf{\Phi}_y$ can be defined as:

$$\mathbf{\Phi}_x = [\mathbf{\Phi}_x^1 \ \mathbf{\Phi}_x^2 \ \cdots \mathbf{\Phi}_x^P] \tag{9}$$

$$\mathbf{\Phi}_y = [\mathbf{\Phi}_y^1 \ \mathbf{\Phi}_y^2 \ \cdots \mathbf{\Phi}_y^Q] \tag{10}$$

where $\mathbf{\Phi}_x^p = \left[e^{-2j\pi p0/M} \ e^{-2j\pi p1/M} \ \ldots \ e^{-2j\pi p(M-1)/M}\right]^{\mathrm{T}}$, and $\mathbf{\Phi}_y^q = \left[e^{-2j\pi q0/N} \ e^{-2j\pi q1/N} \ \ldots \ e^{-2j\pi q(N-1)/N}\right]^{\mathrm{T}}$, $p = 1, 2, \ldots P$, $q = 1, 2, \ldots Q$, respectively. Each pixel of the ISAR image can be denoted as $\mathbf{\Omega}_i(p, q) = \sigma_i(p, q)\exp\{-j\frac{4\pi f_m}{c}z\sin\varphi_i\}$, and each non-zero pixel represents one scattering center located on the target. Generally,

the whole non-zero pixels occupy only a small part of the image plane, which motivates the CS approach to reconstruct $\boldsymbol{\Omega}_i$ from $\mathbf{S}_i$. Considering the additive noise, the ISAR imaging problem can be obtained by solving the following optimization problem as:

$$\min_{\boldsymbol{\Omega}_i} \parallel \boldsymbol{\Omega}_i \parallel_0 \quad \text{s.t.} \quad \parallel \mathbf{S}_i - \boldsymbol{\Phi}_x \boldsymbol{\Omega}_i \boldsymbol{\Phi}_y^{\mathrm{T}} \parallel_{\mathrm{F}}^2 \leq \epsilon \qquad (11)$$

where $\parallel \cdot \parallel$ denotes the number of non-zero components in $\boldsymbol{\Omega}_i$, $\parallel \cdot \parallel_{\mathrm{F}}$ represents the Frobenius norm of a matrix, and ϵ is a small constant which bounds the noise level. Equation (11) can be solved by using a 2D-SL0 algorithm [8], which introduces a Gaussian function to approximate the l_0 norm, and works fast and well toward the 2D signal. The details about this reconstruction algorithm can be found in [8].

By processing each channel independently, a pair of ISAR images is formed, each one corresponding to one of the two antennas (with different elevation angles). The height of each scattering center can then be estimated by using equation (6). It should be noted that since the height estimation is linearly independent of the phase difference between the two ISAR images, it is important to preserve the scatterers phase information in each channel. Unfortunately, the above described independent processing is not able to guarantee that the relative phase is preserved. The main reason for this is that the two images do not necessarily share the same non-zero pixels, i.e. the non-zero pixels may not be present in the same pixel in the two images.

In the following, we propose a method to form the ISAR images with the non-zero pixels consistency, which improves the height estimation performance. Firstly, noting that the two ISAR images share the same sparsity support, that is to say, the scattering centers are located on the same positions in both images, we define the following global-sparsity constraint as:

$$\|\boldsymbol{\Omega}\|_0 = \||\boldsymbol{\Omega}_A| + |\boldsymbol{\Omega}_O|\|_0 \qquad (12)$$

where $\|\boldsymbol{\Omega}\|_0$ stands for the global-sparsity. Equation (12) means that we take the sum of the two images as the common sparsity support, and then we can reconstruct the ISAR images constrained by (12), which can be formulated as:

$$\min_{(\boldsymbol{\Omega}_A, \boldsymbol{\Omega}_O)} \parallel \boldsymbol{\Omega} \parallel_0 \quad \text{s.t.} \quad \begin{cases} \parallel \mathbf{S}_O - \boldsymbol{\Phi}_x \boldsymbol{\Omega}_O \boldsymbol{\Phi}_y^{\mathrm{T}} \parallel_{\mathrm{F}}^2 \leq \epsilon \\ \parallel \mathbf{S}_A - \boldsymbol{\Phi}_x \boldsymbol{\Omega}_A \boldsymbol{\Phi}_y^{\mathrm{T}} \parallel_{\mathrm{F}}^2 \leq \epsilon \end{cases} \qquad (13)$$

where ε is chosen according to the channel with lower noise level to make sure good ISAR images can be obtained for each channel. Since equation (13) is solved by the same sparsity constraint as defined by (12), the reconstructed scattering centers are located on the same pixels in both images, which solves the problem encountered by using the independent processing.

A second definition of the global-sparsity is given by:

$$\|\boldsymbol{\Omega}\|_0 = \|\max(|\boldsymbol{\Omega}_A|, |\boldsymbol{\Omega}_O|)\|_0 \qquad (14)$$

This definition selects the larger amplitude pixels between the two images as the sparsity support, which also solves the
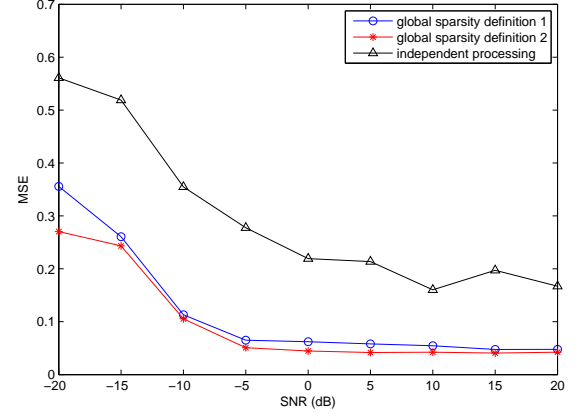

Figure 3: Comparison of height estimation MSE as a function of SNR by different methods. The two elevation angles are $0°$ and $0.057°$

non-aligned scattering centers that appears in the independent processing.

These two global-sparsity constraints guarantee the consistency of the scattering centers in each channel and, as a consequence, the resulting height estimates are more accurate than those obtained with the independent processing.

IV. SIMULATION RESULTS

In this section, simulation experiments are carried out to test the propose method. A target composed of seven scattering centers is simulated, with the scatterers' positions being: (0, 0, 4), (0, 1, 2), (0, -1, 2), (-1, 0, 6), (1, 1.5, 1), (1, 0, 3), and (-0.5, 1.5, 2.5) meters, and each with the same unit amplitude reflectivity function. The carrier frequency of the interferometric ISAR system is 10 GHz, and its bandwidth is 1 GHz with the stepped frequency of 10 MHz. The total rotation angle of the target is $5.7°$ centered on $0°$ in steps of $0.057°$. A pair of antennas with elevation angles $0°$ and $0.057°$ is used to simulate the interferometric radar. Figure 2 shows the 3D reconstruction results by independent processing and joint processing constrained by two global-sparsity definitions. As can be seen, positions of the scattering centers reconstructed by the joint processing are more accurate than those estimated with the independent processing.

In order to evaluate the performance of the proposed algorithm in the presence of noise, Gaussian noise is added into the data with different SNR levels. Figure 3 shows the height estimation MSE result as a function of SNR. It can be seen clearly that the joint processing performs better than the independent processing. Moreover, the global definition #2 seems to give slightly better estimates than the global definition #1.

In order to show the relationship between the height estimation MSE and the elevation angles, the proposed method is evaluated using different elevation angles. In this experiment we fix the antenna O, and adjust the antenna A to make different elevation angles. Figure 4 depicts the height estimation MSE result as a function of different elevation angles. It can be noticed that under different elevation angles, the joint
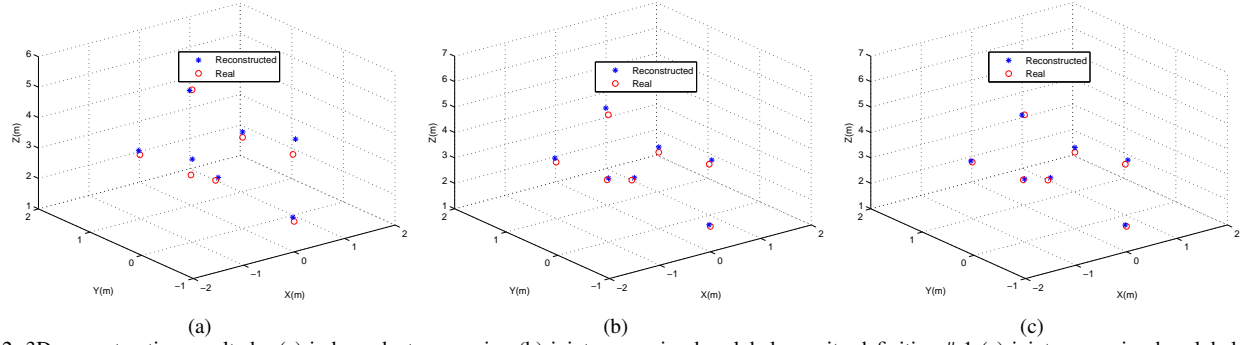
Figure 2: 3D reconstruction results by (a) independent processing (b) joint processing by global-sparsity definition # 1 (c) joint processing by global-sparsity definition # 2.
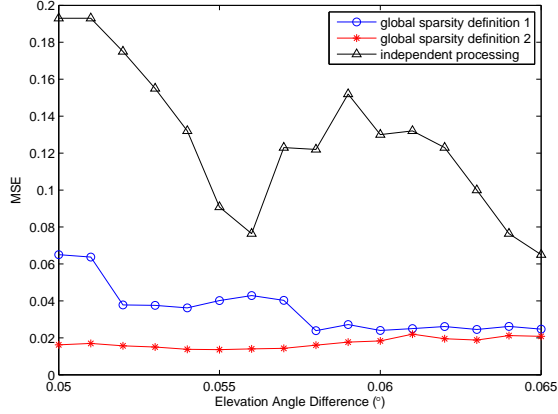

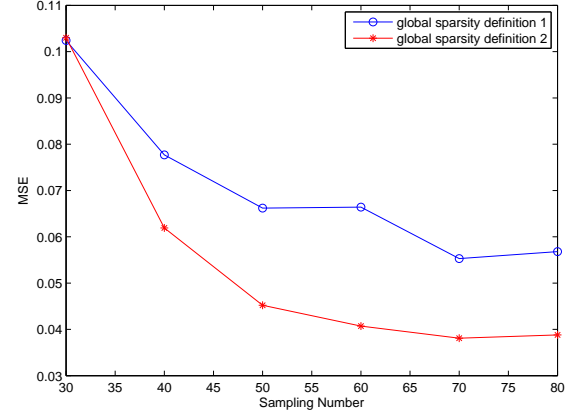Figure 4: Comparison of height estimation MSE as a function of elevation angle difference

Figure 5: Comparison of height estimation MSE as a function of number of samples. The two elevation angles are $0°$ and $0.057°$

processing always outperforms the independent processing.

According to the principle of CS, the sparse signal can be recovered by using limited measurements. In order to show the relationship between the height estimation MSE and number of used measurements, the proposed method is examined using limited measurements. In this experiment, only the joint processing by two global-sparsity definitions are tested, and the numbers of the samples used in the frequency and slow-time domain are the same. Figure 5 shows the height estimation MSE by two global-sparsity definitions when limited measurements are used. It can be noted that the MSE is quite low even only about 25% of the total measurements are used (i.e. sampling number is 50), and in this case global-sparsity definition 2 also performs better than the global-sparsity definition # 1.

V. CONCLUSION

In this paper, we propose a 3D target reconstruction method based on CS. The method makes use of a simple interferometric ISAR system composed of two closely separated antennas with elevation angle offset. Scattering centers in each channel are reconstructed by solving the global-sparsity constrained optimization problem, then the height of each scatterer can be estimated. Simulation results are shown to verify the proposed method. Actually, in real imaging scenario, the target of interest is always non-cooperative, which means the effective rotation vector is not known *a prior*, and thus it

is hard to interpret the 3D images obtained by the two-antenna interferometric ISAR system. The future work will focus on the use of L shape antennas to achieve 3D target reconstruction and effective rotation vector estimation.

REFERENCES

[1] E. Radoi, A. Quinquis and F. Totir, "Supervised self-organizing classification of super-resolution ISAR images: an anechoic chamber experiment," *Journal of Applied Signal Processing (special issues on ISAR),* pp. 1177-1188, Jan. 2006

[2] K. Kim, D. Seo, and H. Kim, "Efficient classification of ISAR images'," *IEEE Transactions on Antennas and Propagation,* vol. 53, no. 5 pp. 1611-1621, May 2005

[3] Xu Xiaojian, R. M. Narayanan, "Three-dimensional interferometric ISAR imaging for target scattering diagnosis and modeling," *IEEE Transactions on Image Processing* , vol. 10, no. 7, pp.1094-1102, Jul 2001.

[4] N. Battisti, M. Martorella, "Intereferometric phase and target motion estimation for accurate 3D reflectivity reconstruction in ISAR systems," *2010 IEEE Radar Conference* , 10-14 May 2010, pp.108-112.

[5] Qun Zhang, Tat-Soon Yeo, Gan Du, Shouhong Zhang, "Estimation of three-dimensional motion parameters in interferometric ISAR imaging," *IEEE Transactions on Geoscience and Remote Sensing,* vol. 42, no. 2, pp. 292-300, Feb. 2004

[6] D. Donoho, "Compressed sensing," *IEEE Transactions on Information Theory*, vol. 52, no. 4, pp. 1289-1306, April 2006.

[7] R. Baraniuk, P. Steeghs, "Compressive radar imaging," *2007 IEEE Radar Conference*, April 2007, pp. 128-133.

[8] A. Ghaffari, M. Babaie-Zadeh, C. Jutter, and H. Moghaddam, "Sparse decomposition of two-dimensional signals," *Proceedings of IEEE International Conference on Acoustics, Speech and Signal Processing*, April 2009, pp. 3157-3160.